GSA DATA REPOSITORY 2012086

Eggenhuisen and McCaffrey

MATERIALS AND METHODS

Set-up

A schematic of the experimental set-up is depicted in Fig. DR1. The experiments were carried out in a 6 m long, 0.5 m wide, 1.5 m deep flume tank. A false floor with a slope of 1° was located 0.8 m below the water table. The open end of this false floor acted as a sump, preventing reflections off the end wall of the tank. A 5.25 m long, open-top channel with a rectangular cross-section 0.2 m wide and 0.5 m high was suspended on the false floor on blocks. A 35 dm3 sediment-water mixing box (350*350*286 mm l*w*h) was positioned above the water table near the start of the channel, so that the top fluid level was 450 mm above the flume water level when filled. A ball valve closed off a vertical pipe; a 90° elbow add-on directed the flow in the down slope direction at the channel floor. The outlet was centred in the middle, at 520 mm from the back and 4730 mm from the downstream end of the channel. Upon opening of the valve, the mixing tank drained under gravity in approximately 15 s. All instrumentation was located in the last 0.75 m of the channel, so that drainage of the sediment water mixture was complete before the flow reached the measurement section and vibrations from the drainage system did not interfere with the pressure signature of the flow.

Sediment

Oakamoor HPF6 grade silica flour with a median grainsize of 9.3 μm was used as sediment in all runs (D10=1.4 μm; D90=29.5 μm). The four mixtures that were used had initial excess densities of 20, 40, 60, and 80 kg/m3.

Experimental Series

In series C1 the concentration of the flows was measured in the measurement section with three Ultra High Concentration Meter (UHCM) probes (5, 42 and 145 mm above the bed and 385, 515 and 680 mm upstream from the channel end respectively; Fig. DR1B-i). In series F1, the channel was entirely empty (Fig. DR1B-ii). For series P1, a circular pole with 20 mm diameter was mounted vertically in the centre of the channel, with the upstream side of the pole 364 mm from the channel end, just downstream of the pressure measurement locations (Fig. DR1B-iii). At 20 mm above the channel floor, a velocity probe was inserted through a hole in this pole, facing upstream. Basal pressures were measured in series F and P, but not in series C because the introduction of the UHCM probes interferes with the pressure field. The inner diameter of the pressure ducts was 5 mm and the centre-points of the three ducts measuring the pressure at the channel base were located 2.5, 21 and 196 mm upstream of the pole.

Instrumentation

Basal pressure measurements were conducted with three differential pressure meters based around Honeywell 20PC differential pressure transducers. Cavities in the housing at both sides of the transducer were filled with water and connected to the experimental flume by two water filled ducts; one was introduced through the channel floor, so that its end was exactly flush with the floor surface; the other ended outside and 1-3cm below the suspended channel. According to Pascal's law, the pressure in two points at the same level in a static fluid in a connected vessel is the same, irrespective of the shape of the vessel. Therefore the precise shape, orientation and elevation of the reference duct exit is irrelevant; the differential pressure between the two pressure transducer ports is equal to the excess pressure (over the clear-water hydrostatic gradient) at the base of the flow. The ends of the hydraulic ducts were shielded by a nylon mesh with 1 μm openings to permit communication of fluid pressure between the base of the experimental flows and the hydraulic ducts connected to the pressure meters, while keeping the sediment laden fluid out of the pressure meter set-up. Some 5.5% by volume of the used sediment was finer then this mesh opening size, yet no sediment was observed to intrude into the measurement system. The pressure meter output is an analogue DC voltage signal that was digitised to a 1 kHz digital signal with an InstruNet data acquisition system. The output voltage has been calibrated to [Pa] (see "*Pressure Transducer Calibration*"; below). The voltage output was found to be linearly dependent on differential pressure and the standard deviation of voltage change per calibration run was 0.9-2.1%.

Fluid velocities were measured with Ultrasonic Doppler Velocity Profiling (UDVP)8 produced by MetFlow. 4 MHz transducer probes were used with settings such that the velocity was measured in 128 bins in front of the probe, each 0.74 mm long, with a measurement frequency of 125 Hz.

Concentration was measured with Ultra High Concentration Meter (UHCM) probes produced by WL-Delft Hydraulics. The output voltage of the probes was digitised and logged with an InstruNet data acquisition system. Each probe was calibrated in a separate calibration program, using similar grade silica flour as in the experiments. Uncertainties derived from calibration runs range from +/- 0.8-1.1% for the three probes. For the determination of the depth averaged excess density, a density profile is defined from these three measurement points and the two gradients. The inflection between the lower and upper gradients in density was placed not at the middle UHCM probe height but halfway between the middle and upper probe, so as not to underestimate the density contribution of the lower high density zone. The data are extrapolated linearly towards the bed and towards a height at which the excess density is 0 kg/m3. The shape uncertainty of the concentration

profile is larger than the measurement uncertainty of individual probes and is estimated at +/-5%.

Pressure Transducer Calibration

Figure DR2 shows 20 seconds of raw pressure transducer data obtained before the start of the first calibration series. Mean and standard deviation of the 20,000 data-points are given in Table DR1. The standard deviation of all four transducers lies in the range 0.01-0.02 V. The drift in the data is determined by subtracting the mean of the 1,000 data-points between 0 s and 1 s from the mean between 19 s and 20 s (Table DR1). PT1 has the largest drift in this measurement with a difference of 0.024 V, which is 1.4 σ. This explains the relatively larger standard deviation of the PT1 time-series (Table DR1). The drift in the other three transducers is much smaller at 0.5 σ, 0.1 σ and 0.1 σ respectively for PT's 2, 3 and 4. The 1 kHz frequency is over-sampled for the needs of the present study, since all other data-types are collected at much lower frequencies (UDVP: 91-125 Hz; UHCM: 10 Hz; Video: 12.5-25 Hz). The present set-up involves transmission of fluid pressures through tubes of approximately 2 m length. If the propagation velocity of the pressure fluctuations is 1.5 km/s, this means that the lag time is larger then the sampling time. In truth the propagation of the signal will take longer due to interaction with the tube wall. There is also no control over the diffusion and interaction of the highest frequency components of the signal as it is transmitted through the hydraulic tubes. Because of these restrictions on the present pressure measurement set-up, it has been decided to perform a moving window averaging on the pressure data. Each data-point in the time-series is replaced by the average of that point and the four data entries on either side, so that the new time-series represents the average pressure over 9 ms, which is comfortably longer than the time necessary for pressure signals to reach the pressure meters. The standard deviations of the smoothed data is reduced with respect to the raw data (Table DR1).

Calibration procedure. In order to determine the calibration function of output voltage to pressure, the channel-base ports of the pressure transducers were set up just as in the experiments described in the main paper. However, the reference port of each pressure meter was not led into the flume, but attached to the outside wall of the flume and filled with water up to the level to which the flume is normally filled at the start of an experimental run. The flume itself was filled to this level and the pressure transducer zero levels were adjusted so that the output signals were in the central portion of the measurement range of -5/+5 V. Water was now drained from the tank until the lowest of the four PT output signals was still just above the bottom of the measurement range. The differential pressure was now negative. The sediment mixing box was filled with 30 dm^3 of clear tab water. A 60 s measurement was started on the data-recording PC with the external battery-powered trigger-circuit and after 5-15 s, the valve of the mixing box was opened, so

that the water drained into the tank, raising the water level. This procedure was repeated four times until the water level in the tank had risen so far above the reference port level that the positive differential pressure caused some or all of the PT output signals to exceed +5 V. This entire calibration series has been carried out four times.

Figure DR3 shows the four time-series obtained from one of the increments in calibration series 4. At the start of the measurement the voltages were constant after an initial perturbation of the rig containing the PT's, which was caused by starting the measurement, had died out. At approximately 10 s the mixing box was opened and the water started to drain into the flume. This set up a number of surface waves that travelled along the flume. At approximately 16 seconds, a short disturbance was picked up that is a typical effect of someone slamming the laboratory door or touching the flume tank or pressure rig (such a disturbance is also present in experiment P1, which is described in the present paper). The water level rise ceased after approximately 15 s when the output voltages reached a plateau. The effect of the waves created by the water draining into the flume diminished during the remainder of the measurement. Note that the pressure effects of the rising water level and possible associated waves are not incorporated in the experiments described in the main text. In those experiments, the reference port is located inside the flume at the same longitudinal position and approximately the same depth as the appropriate channel-base port, so that the pressure signal from the free-surface elevation changes is equal in both ports and is not picked up by the pressure meters.

Calibration results. From the 16 measured increments, the increase in voltage was determined by subtracting the mean of the initial stable values (from ~2 to ~9 s) from the mean of the values after the drainage of the tank (from ~35 to 60 s). The voltage increments of the four PT's are plotted in Fig. DR4. Some of the voltage increments can be seen to be off-set from the general trends. For PT2, both calibration series 1 and 2 were performed with failing batteries. The same problem is affecting PT1 during calibration series 3. The output from PT4 has exceeded +5 V during the final increment of calibration series 1 and 2. These anomalous values (indicated with a red dot in Fig. DR4) have been disregarded in the present calibration.

It is assumed that the average of the wave affected voltages represents the average water level. By repeated measurement of the water level increase with a mounted ruler, it was determined that the water level increase resulting from the drainage of the mixing box was 8.5 mm. This yields a differential pressure increase of 83.3 Pa (with: ρ_{water}=999 kg/m^3; g=9.81). Table DR2 shows the average voltage increase over all successful measurements for the 4 pressure transducers, the standard deviation of the voltage increases (both absolute

and relative) and the resulting calibration constant relating voltage increases with the rise in pressure in the flume.

Calibration uncertainty. Two uncertainties have been described above: one due to fluctuations of output voltages around a mean value even under constant experimental conditions (Table DR1) and one associated with the calibration constant (Table DR2). The first uncertainty can be recognised in the small timescale fluctuations around a local mean in the time-series incorporated in the main part of our paper. Since sections of data lasting for several seconds are used to determine average values for the pressures presented in Figure 4, the error associated with this uncertainty averages out. The error associated with the calibration constant varies between 0.9 and 2.1% (Table DR2), which is considered satisfactorily for the present purposes.

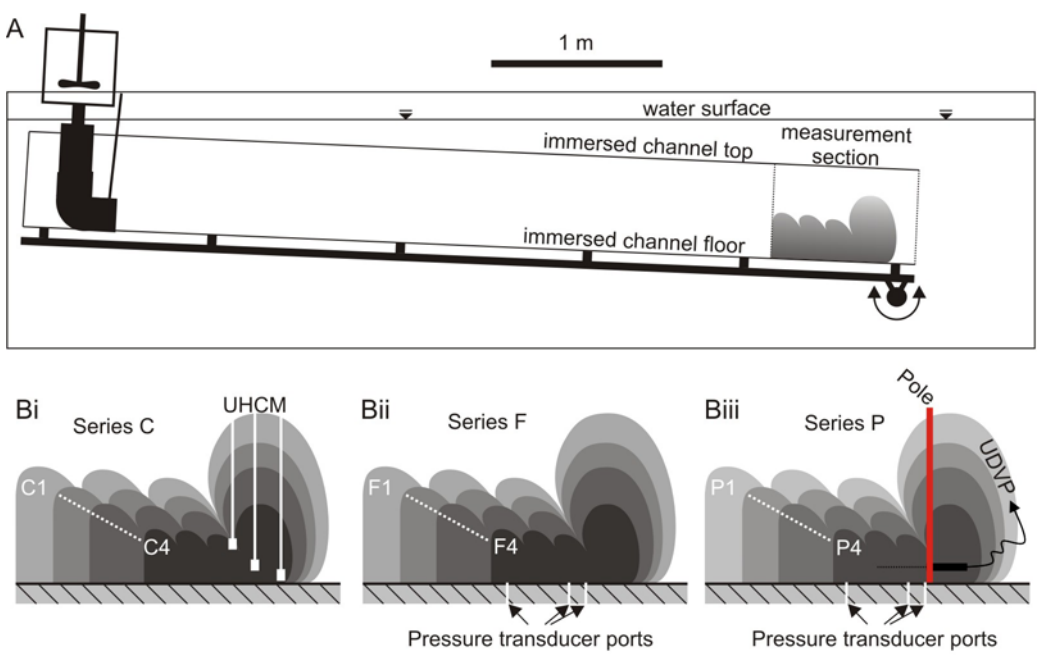

Figure DR1. Schematic set-up and boundary conditions of series C, F and P.

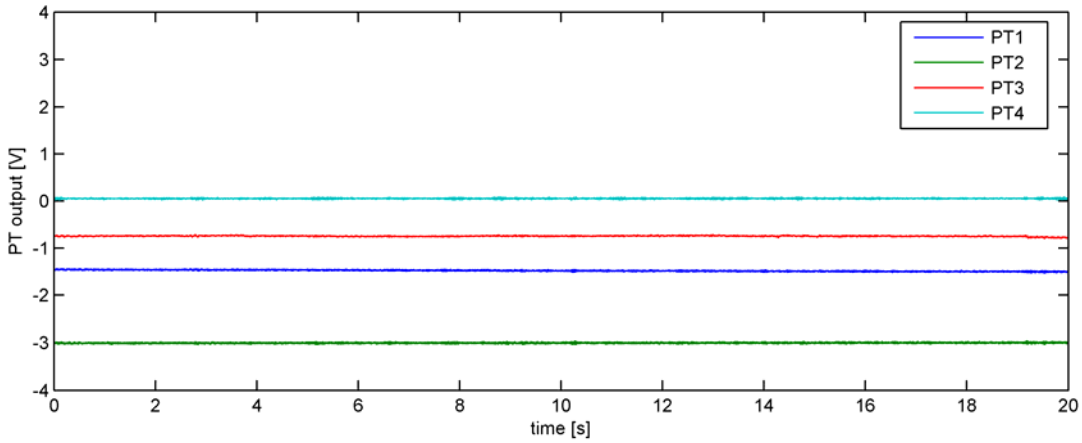

Figure DR2. 20 seconds of recorded data before the start of calibration series 1.

PT #	Mean [V]	σ (1 kHz) [V]	Drift [V]	σ (smooth) [V]
1	-1.48	0.017	-0.0242	0.015
2	-3.00	0.012	0.0064	0.008
3	-0.75	0.011	0.0010	0.010
4	0.050	0.012	0.0015	0.010

Table DR1. Statistics of recorded data shown in Fig. DR2. The mean voltage, standard deviation of the raw data, drift during the 20 s measurement and standard deviation after time averaging.

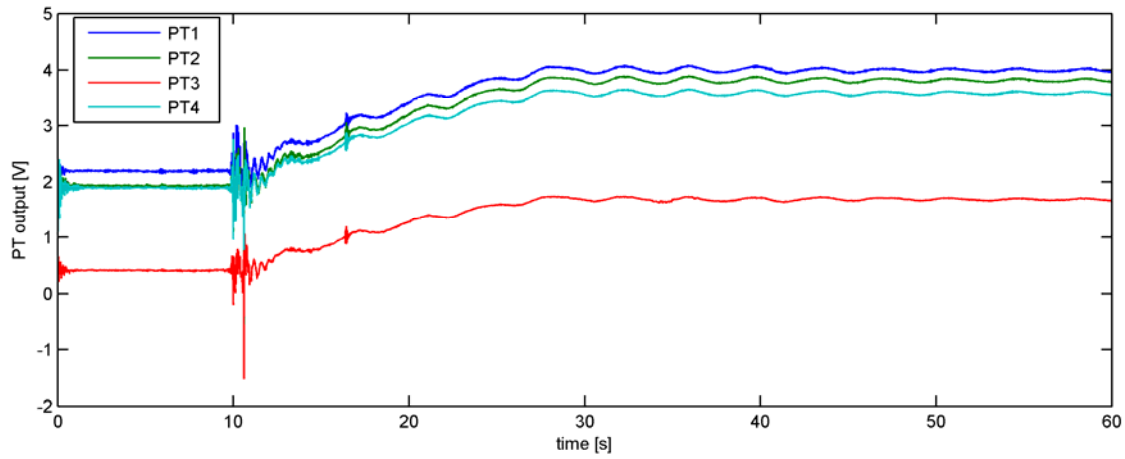

Figure DR3. A 60 s time-series of PT output voltages obtained during a calibration increment in calibration series 4.

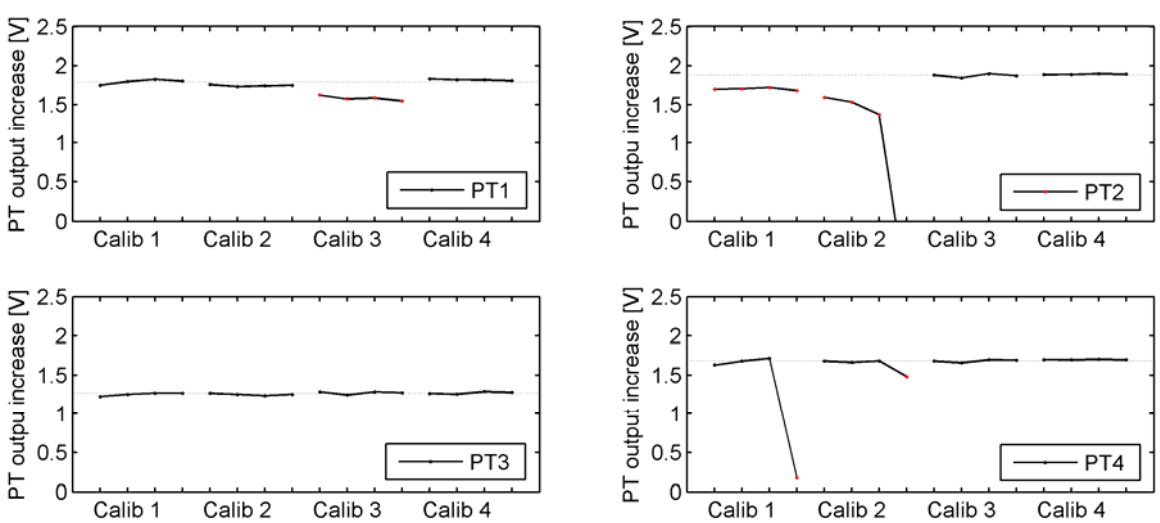

Figure DR4. Output voltage increases for the 4 calibration increments of the 4 calibration series for the 4 pressure transducers.

PT #	Mean inc. [V]	σ inc [V]	σ inc [-]	Calib C [Pa/V]
1	1.79	0.037	0.021	46.6
2	1.88	0.017	0.009	44.2
3	1.26	0.018	0.015	65.9
4	1.69	0.022	0.013	49.4

Table DR2. Calibration results for the 4 pressure meters. Second column displays the mean voltage increase of all calibration increments indicated with a black dot in Fig. DR4. Standard deviations are given both in absolute voltages and normalised with the mean. The calibration constants in the last column are the constants used in processing the data presented in the current paper.